

Template-less Quasi-Rigid Shape Modeling with Implicit Loop-Closure

Ming Zeng* Jiaxiang Zheng Xuan Cheng Xinguo Liu†
State Key Lab of CAD&CG, Zhejiang University

Abstract

This paper presents a method for quasi-rigid objects modeling from depth scans which are captured at different time instances. The quasi-rigid object, such as a human body, hardly keeps fully still when a depth camera moves around the object to capture depth scans from different views. Our method adopts a model-to-part way to gradually integrate sample nodes of depth scans into a deformation graph and then update it. Under the as-rigid-as-possible assumption, the model-to-part way is able to adjust the deformation graph non-rigidly so as to avoid obvious alignment error accumulation, which also exhibits implicit loop-closure. To help the deformation graph be flexible to adjustment against drift and topological error, two key algorithms are designed. For the registration, we use a two-stage registration to largely keep the rigid motion part. For the integration and update, we dynamically control the regularization effect in a topological-aware way.

We illustrate the effectiveness and robustness of our method on several depth sequences of quasi-rigid objects. We also show the result of human shape modeling as an application of our method.

1. Introduction

It's very important in computer vision to reconstruct surface of 3d objects. With the recent developments of stereoscopic vision and depth acquisition devices, it becomes possible to obtain the 3D models using images or depth scans from different views. To capture image/depth scans from different views, one way is to utilize multi-sensors to capture the object in one-shot (e.g. [7, 24]). This kind of methods require sufficient amount of spatially arranged cameras. A cheaper way is to move a sensor around and capture the object from multiple directions (e.g. [9, 15]). This method, however, is limited to static objects. Nevertheless, most objects are unable to keep static during the capturing procedure, e.g., human body with some deformable shapes, as is illustrated in Figure 1.

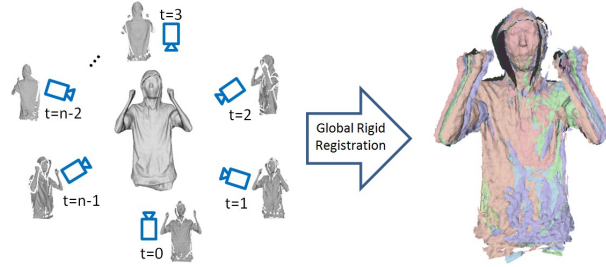


Figure 1. The quasi-rigid object exhibits slight deformation, which can not be reconstructed in a rigid registration fashion.

Using a single camera to capture the whole shape of non-rigid objects is a deformable shape completion problem. Deformable shape completion problem is general ill-posed due to lacking of information from the opposite side at each time instance. Recently, kinds of priors are used to cope with the under-constraining. The template based methods (e.g. [10, 23]) confine the shape on un-seen views in the template space by sacrificing the generality of these methods. The color images based methods (e.g. [13]) utilize the salient feature points on color images to track correspondences, but they heavily rely on the robust feature tracking. The space-time methods (e.g. [14]) assume the locally continuous movements by requiring a sufficiently dense sampling on the time axis. Articulated models (e.g. [5]) reduce the freedom of the deformable objects, which leads to missing of details. There are more general methods (e.g. [25, 22]) which leverage few assumption on specific area, but these methods take little care about loop-closure, a crucial issue on object reconstruction.

In this paper, we aim at tackling the deformable shape completion problem with nearly rigid objects, and we call them quasi-rigid shapes. At the as-rigid-as-possible scenario, we are able to complete the model visually-plausibly without the assist of a template. Furthermore, thanks to the freedom reducing brought by the quasi-rigid assumption, our pipeline is much simpler than previous method. We maintain a graph which represents sampling of the object during the whole pipeline, and adopt an incrementally integration way to update the graph. For each depth scan,

*mingzeng85@gmail.com

†Corresponding author. xgliu@cad.zju.edu.cn

the graph is registered to it in a model-to-part way. The model-to-part way with the non-rigid deformation model is flexible enough to gradually adjust the graph to new depths, and is able to achieve the loop-closure requirement naturally. After registration, the depth scans are sampled and integrated into the graph. The integration is with much care on topology, and provides topology-aware information for regularization on the registration step of successive scans. After integrating all depth scans, a global nonrigid warping is adopted to warp points to their destination positions in the last frame. And finally, we use poisson reconstruction to fuse and extract the object’s surface.

The key contribution of this paper is a method to obtain the 3D models of quasi-rigid objects in a template-less way while implicitly keeping the loop-closure. The method consists of the following technical contributions:

- Firstly, we propose the model-to-part registration scheme with the non-rigid deformation to flexibilize the integrated model, which distribute the accumulated error in each registration step, avoiding explicit steps for error distribution like previous methods.
- Secondly, we introduce the two stage registration method to make the registration step robust to geometry tracking.
- Thirdly, we propose several practical schemes for the correspondences and topological issues, which largely improve the robustness of the method.

2. Related Work

Rigid Registration. To obtain the whole 3D model of a static object, scans of different views should be aligned together in a common coordinate by undergoing rigid transformations. Rigid Registration find the rigid transformation between two scans. Iterative closest point (ICP) [2, 6] is a framework to solve the problem, which finds point correspondences by nearest neighbor criterion, and finds a rigid transformation by minimizing a energy function which sums up distances of these correspondences, and repeats the process until convergence. There are several variants [17] of the original ICP, which mainly focus on the correspondences finding and the distance metrics. The rigid registration is unable to deal with non-rigid shape, but it is robust due to its low freedom, and the property can be leveraged in our quasi-rigid case.

Non-Rigid Registration. For deformable shapes, more freedom is needed to represent the deformation of shapes. Based on the embedded deformation introduced by Sumner et al. [19], Li et al. [12] combine the correspondence optimization with deformation optimization together, and increase the robustness of registration. Based on the same deformation model, Huang et al. [8] studied the problem

under isometric deformation, and argued that keeping low but necessary deformation freedom will improve the registration reliability. With the similar principle to reduce deformation freedom, Chang and his colleagues introduce an articulated model [3] and a linear blend skinning model [4] for the nonrigid registration. These pairwise registration methods are necessary building blocks for the whole shape reconstruction.

Shape Completion The shape completion problem requires merging scans from different views to reconstruct the whole shape. To cope with the unreconstructed problem, kinds of prior are incorporated to confine the shape in a subspace. Li et al. [10] leverage a coarse template to track the movement of the depth scan. Weiss et al. [26] reconstruct human bodies with a parameterized human model SCAPE[1]. Using this Scape model, Tong et al. [23] pairwisely track the scans from slightly moving human, and impose a explicit global alignment to distribute the accumulated alignment errors. These methods require template beforehand, which limits the generality of these methods. Liao et al. [13] proposed a template-free method, which assumes a locally continuous movement and track the correspondences on associated RGB images. The method will fail when the RGB images is noisy or absent. The Space-time methods (e.g. [14, 20]) take the same locally continuous condition by requiring a sufficiently dense sampling on the time axis. These methods optimize the registration problem in a small window of multiple frames to avoid an additional error distribution step. Chang and Zwicker [5] restrict the moving shape be articulated, and solve the joint labeling/deformation problem with the reduced deformation model. But the method will lead to missing details on more deformable objects, e.g. the folds of cloth. Wand et al. [25] and Tevs et al. [22] proposed more general frameworks which impose few assumption on specifical area. These methods are mainly designed for capturing a sequence of moving objects, therefore, they take little care about loop-closure.

Our model-to-part way is similar to temporally coherent completion [11] proposed by Li et al. The incremental integration way may incur error accumulation in the rigid case, but the scheme works fine in the nonrigid case thanks to the adjustability of the pre-integrated models. Unlike the multi-view scenario in [11], we deal with single-view completion problem, which is more liable to fail due to topology issues. In our paper, we study the model-to-part way further than [11] by incorporating the topology information obtained from the integration step into pairwise registration step, which adaptively control the flexibility of the integrated model.

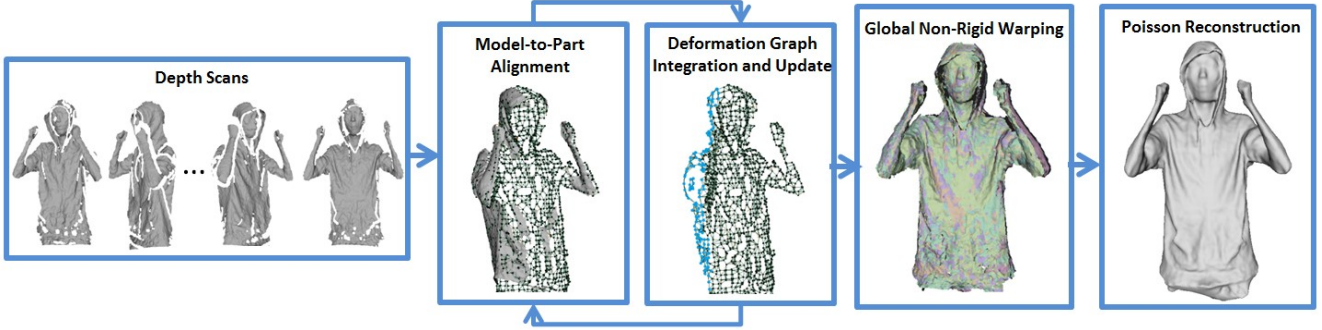


Figure 2. Overview. A deformation graph is non-rigidly registered to each new depth scan, which is followed by the integration and update of the deformation graph. After integration of these depth scans, a global non-rigid warping is conducted on each scan according to the deformation records of this graph. Finally, the resulted mesh model is obtained by poisson reconstruction.

3. Overview

Figure 2 gives the overview of our method. The input is a sequence of depth scans of a quasi-rigid object captured from different views at different time instances. These depth scans are inserted into our pipeline one by one. When a scan comes, a deformation graph is non-rigidly registered to it, and then the new part brought by this new scan is sampled and integrated into the deformation graph. Then the topology of this deformation graph is updated. The registration and the integration/update procedures iteratively execute until the end of the sequence. After all depth scans are processed, the deformation graph records the whole deforming/dynamic behaviors of the scanned object together with the poses of the depth camera. Using this dynamic information, all depth scans are aligned into one global coordinate and register together to offset slight deformation of the quasi-rigid object. Finally, poisson reconstruction is used to build the mesh model.

In the rest of this paper, we will first introduce the model-to-part registration in Section 4, deformation graph integration and update in Section 5, then we present the implementation details and the experimental results in Section 6, and conclude this paper in Section 7.

4. Model-to-Part Registration

In the rigid alignment scenario, there is inevitable accumulation error without a global registration [16, 18]. A model-to-part scheme [21] incrementally align a new scan into a integration model, which improve the alignment of the new scans, but it is unable to adjust the integrated model. Recently, Newcombe et al. adopted a model-to-part way in their proposed KinectFusion [15] to incrementally integrate new scans. They argued that in their algorithm, alignment error will be eased thanks to the constantly update of the integrated model. Inspired by KinectFusion, we take a similar way in our quasi-rigid registration case. In our method, the

integrated model is able to be “moved” and “dragged” to match the new scan, and updates its shape iteratively. Furthermore, as is illustrated in Figure 3, the relatively flexible way inherently keeps loop-closure by adjusting the “head” and the “tail” of integration model to match the last scan together.

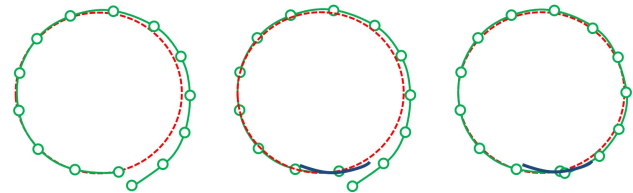


Figure 3. Illustration of implicit loop-closure of model-to-part registration. The red is ground truth, the green is deformation graph, and the dark blue is a depth scan. left: the registration suffers from slight drift. middle: the new scan overlaps with the first scan. right: model-to-part registration adjusts the deformation graph as rigid-as-possible, which exhibits loop-closure implicitly.

4.1. Deformation Model

For the moving object, it is with two kinds of transformations [12]: global rigid transformation Φ_{global} and local non-rigid deformation Φ_{local} . The global rigid transformation is because of camera movement or the object’s entire movement. The local non-rigid deformation comes from slight articulated motion or the low-scale deformation therein (such as folds in the cloth). Therefore, for a point at position p_i , its transformed position

$$\tilde{p}_i = \Phi_{local} \circ \Phi_{global}(p_i) \quad (1)$$

and

$$\Phi_{global}(p_i) = Rp_i + T, \quad (2)$$

where R is a 3×3 rotation matrix and T is a 3×1 translation vector.

For the local non-rigid deformation, we use the embedded deformation model [19], where a node s_j in the deformation graph determines a local warping field to control the transformation of points near s_j . A 3×3 matrix H_j and a 3×1 translation vector l_j are used to represent such a local deformation:

$$\Phi_{local}(p_i) = \sum_{j=1}^k w_{ij} [H_j(p_i - s_j) + s_j + l_j], \quad (3)$$

where the normalized weights w_{ij} for p_i 's k-nearest nodes $s_j, j = 1, 2, \dots, k$ is defined as:

$$w_{ij} = \frac{1 - \|p_i - s_j\|/d_{max}}{\sum_{m=1}^k 1 - \|p_i - s_m\|/d_{max}}. \quad (4)$$

with d_{max} is distance between p_i and its $k+1$ th nearest node.

4.2. Two Stage Registration

For the deformation graph G_t at frame t , the way to register to the next scan D_{t+1} , is to find the best transformation $\Phi = \Phi_{local} \circ \Phi_{global}$ that fits G_t and D_{t+1} well, while keep the deformation locally rigid and locally smooth.

Following the optimization way proposed by [19], a fitting term E_{fit} , a rigidity terms E_{rigid} , and a regularization term E_{reg} are combined together to form a minimization problem:

$$\min_{R_t, T_t, A_t^i, l_t^i, i=1,2,\dots,|G_t|} E_{fit} + w_{rigid} E_{rigid} + w_{reg} E_{reg} \quad (5)$$

In the function, $E_{fit} = \sum_{i=1}^n M(\Phi(s_t^i), d_{t+1}^i)$ serves as the fitting terms. d_{t+1}^i is node s_t^i 's correspondence in D_{t+1} , and $M(x, y)$ is some distance metrics (see below). $E_{rigid} = \sum_{i=1}^n Rot(H_i^k)$ where $Rot(H) = (h_1' h_2)^2 + (h_1' h_3)^2 + (h_2' h_3)^2 + (1-h_1' h_1)^2 + (1-h_2' h_2)^2 + (1-h_3' h_3)^2$ and h_1, h_2, h_3 are H 's column vectors. E_{rigid} ensures the affine transformation to be near rotation. $E_{reg} = \sum_i \sum_{j \in N(i)} \|H_t^i(s_t^j - s_t^i) + s_t^i + l_t^i - (s_t^j + l_t^j)\|^2$ specifies the smoothness of the neighboring deformation.

It's able to solve all unknown variables altogether in Eq.5. However, specifically for the quasi-rigid object, Φ_{global} accounts for most of the motion. Based on this point, we treat the rigid part and the non-rigid part separately, and propose a two stage registration strategy. We first view the graph G_t as totally rigid, and solve the global transformation R_t and T_t in a rigid stage. Following is a non-rigid stage, we further solve the optimization problem in Eq.5 given the determined R_t and T_t .

Rigid Registration Stage: We adopt Iterative Closest Point [2, 6] to estimate rigid transformation between G_t and D_{t+1} . And the fitting energy E_{fit} combines the point-to-point and point-to-plane metrics:

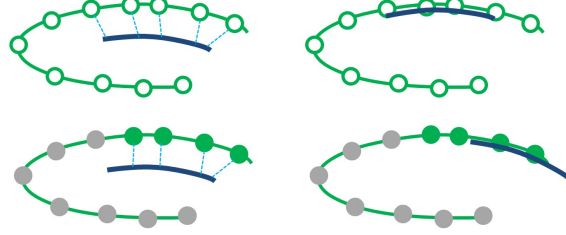


Figure 4. Illustration of subset registration. top left: the full-set correspondences introduce wrong correspondences, leading to bad alignment (top right). bottom left: the subset correspondences (green) masks the outdated nodes (grey), leading to expected alignment (bottom right).

$$E_{fit} = \sum_i \|R_t s_t^i + T_t - d_{t+1}^i\|^2 + \rho \|n_i'(R_t s_t^i + T_t - d_{t+1}^i)\|^2 \quad (6)$$

Where, n_i is normal with d_{t+1}^i . The correspondences which are far apart or normal incompatible are pruned [17]. We use $\rho = 0.1$ for our experiments.

As the scans are integrated into the deformation graph, nodes added in the very beginning of the integration procedure do not overlap with the new scan. These outdated nodes will disturb the registration due to introducing wrong correspondences. Therefore, we adopt a subset registration scheme. After registration of previous scan, we record the nodes which are covered by the previous scan, and mark them as active nodes. At the start of the registration of new scan, we only use the active nodes while mask the outdated nodes in the rigid registration. As is illustrated in Figure 4, the scheme improves the robustness of the rigid registration, especially for the graph having integrated lots of scans.

Non-Rigid Registration Stage: Given the rigid transformation R_t and T_t from rigid registration stage, we optimize the Eq.5 to obtain the local transformations for each nodes in the deformation graph. Like rigid registration, we adopt point-to-point and point-to-plane metrics together in E_{fit} , which ensures the non-rigid registration flexible enough to globally “slide” on the target scan. Similar to [19], the optimization Eq.5 can be minimized using Gauss-Newton algorithm.

In the quasi-object case, since the object's non-rigid deformation is slight, there is no necessary to register in an explicit coarse-to-fine way. We deal with the over-flexibility problem by a simple method which is composed of two points. The first, we set a large weight w_{reg} to keep the deformation as-rigid-as-possible. In our following experiments, we use the weights $w_{reg} = 10^4$, $w_{fit} = 10^2$, and $w_{rigid} = 1$. The second, to prevent the deformation graph from gathering together, we take a bijective closest correspondence instead of one-direction closest correspondence. Specifically, for a node s_i with normal n_{s_i} belonging to the

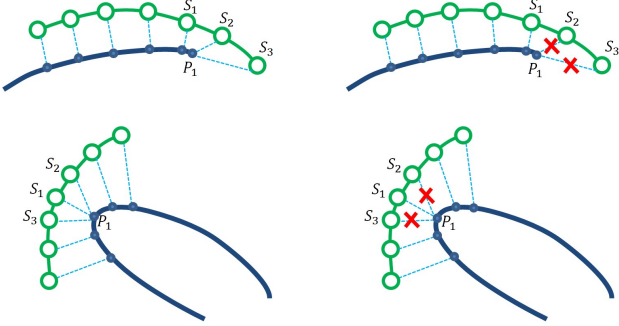


Figure 5. Bijective closest correspondence. Top left: (s_2, p_1) and (s_3, p_1) are wrong, because $\text{Near}(p_1)$ is neither s_2 nor s_3 . The wrong correspondences will lead s_2 and s_3 to gather to p_1 . Top right: The wrong “edge point” correspondences are pruned. Bottom: similar to top. But here is “tip point” case. left: failing to prune wrong correspondences leads s_1 , s_2 , and s_3 to gather together. right: the wrong “tip point” correspondences are pruned.

set of graph nodes S , suppose its nearest point on a depth scan is p_i^* with normal $n_{p,i}^*$, we find the id of p_i^* 's nearest normal-compatible point $\text{Near}(p_i^*)$ from S :

$$\begin{aligned} \text{Near}(p_i^*) &= \arg_h \min \|p_i^* - s_h\|^2, \\ \text{s.t. } &\arccos(n_{s_h} \cdot n_{p_i^*}) < \pi/3 \\ &\|p_i^* - s_h\|^2 < \text{threshold} \\ &s_h \in S \end{aligned} \quad (7)$$

When $\text{Near}(p_i^*)$ equals to i , the correspondence (s_i, p_i^*) is valid, otherwise it is pruned. As shown in Figure 5, the bijective closest correspondence can prune wrong “edge point” and “tip point” correspondences.

5. Deformation Graph Integration and Update

The deformation graph is gradually built up as depth scans are inserted into our pipeline. At the first scan, we directly use the sampled points from the depth scan as the nodes of the deformation graph. The nodes with the edges between nearest neighbors form the graph. In our experiments, we set the edge count $k = 6$ for each nodes. When a new scan is inserted, we register the deformation graph to the scan, and then add sample nodes into graph and update the topology.

5.1. Feature Preserving Sampling

Our method samples nodes from scans by a combination of uniform sampling in point position and uniform sampling in normal space [8]. The uniform sampling ensures the nodes cover all region of the scan, while the normal space sampling makes sure features on the scan are equally sampled.

5.2. Topological-Aware Integration

For each sample points $S_{t+1} = \{s_{t+1}^i\}$ from depth scan D_{t+1} , if its distance to the nearest point in the deformed graph \tilde{G}_{t+1} exceeds a threshold (0.05), it is added into the graph. The simple method works fine on most cases, but fails on some scenarios which need special cares on topological issues. One example is two sides of a thin cloth. Another case is a re-appearing part which re-appears in a position very close to its another side. We treat the topological issues by considering normal directions. For the sample points which are near the graph nodes, but with a normal in different direction (angle > 150), it should be added into the graph as well.

5.3. Relax-Regularization for Re-appearing Parts

After new sample points are added into the deformation graph, the nodes’ nearest neighbors are recomputed and their edges are rebuilt. According to the topological-aware integration, two neighboring nodes in the graph may have very different normals. It may result from the two opposite sides of a thin part as mentioned in the previous subsection, or arises when a disappeared part suddenly re-appears in the camera view.

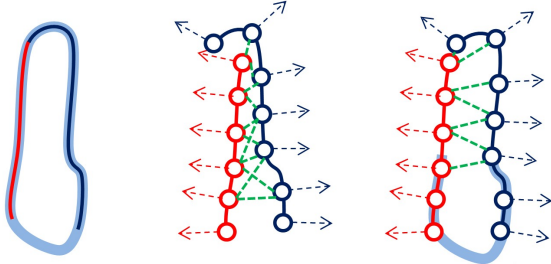


Figure 6. Illustration of relax regularization. Left: ground truth of a shape. Middle: the shape suddenly re-appears, and there is a large gap between the current scan (dark blue) and the previous scan (red), the relax regularization sets weak influences between them (green dash line). Right: the relax regularization allows these two parts move apart when the graph are registered to new scans which have large overlapping regions between both red and dark blue parts.

In the re-appearing case, the re-appearing parts may fail to match the previous scans well due to little overlapping area between them. Since these two parts may belong to a same articulated component and should move together, it’s reasonable to link the nodes from these two parts with edges for the registration regularization E_{reg} . However, the influence between nodes with incompatible normals should be weaker than that of normal-compatible nodes, so as to allow the bad alignment to be adjusted to correct positions. We illustrate this case in Figure 6. Based on the consideration, we relax the regularization between position-near

but normal-incompatible nodes by introducing a relax regularization controller. Mathematically, for two sample nodes s_t^i and s_t^j , the relax regularization controller $c_{reg}^{i,j}$ between them is defined:

$$c_{reg}^{i,j} = \begin{cases} c_{high}, & n_i \cdot n_j > 0 \\ c_{low}, & n_i \cdot n_j \leq 0 \end{cases} \quad (8)$$

In our experiments, we set $c_{high} = 1$ and $c_{low} = 0.1$.

With the regularization controller, the regularization term E_{reg} is rewritten as:

$$E_{reg} = \sum_i \sum_{j \in N(i)} c_{reg}^{i,j} \cdot \|H_t^i(s_t^j - s_t^i) + s_t^i + l_t^i - (s_t^j + l_t^j)\|^2. \quad (9)$$

6. Experiments

We have tested our method on a serial of real depth data. We captured 640×480 depth data by moving a Kinect around objects, or moving objects around the Kinect. The frame rate of the capture is 30 fps. However, since our method does not require dense sampling at the time axis, we uniformly sampled the data and only kept 10 to 15 frames (each frame covers about 24 to 36 degrees) for reconstruction.

All the pipeline are implemented with C++, and tested on an desktop computer with Intel Core2 Duo E7400 2.80GHz CPU (one core used) and 2GB RAM. In all the experiments, the rigid registration converges within 30 iterations and the non-rigid registration converges within 10 iterations, which costs about 20 seconds for a frame. The graph integration and update is very fast, which cost about 1-2 seconds for a frame. The whole pipeline takes 5-7 minutes to finish a model, regarding to the number of scans.

6.1. Comparisons on Each Proposed Techniques

In this subsection we show the effectiveness by leaving some feature out, and comparing it with the all-features-equipped pipeline.

Two Stage Registration. We compare our two-stage-registration and only-nonrigid-registration. As is shown in Figure 7, (a) and (b) are two views of initial position before registration. (c) is the result using nonrigid registration only. The alignment on the hand is stuck in local minimal. The two-stage-registration first rigidly register the graph to the scan (d) to obtain a good initial position, and then nonrigidly register to get the fine result (e).

Bijective Correspondence. Figure 8 demonstrate the effectiveness of the bijective correspondence. Without the bijective consistence, the graph nodes on the foot shrink to the joints (Figure 8(a)). While the bijective consistence prevents the gathering phenomena (Figure 8(b)).

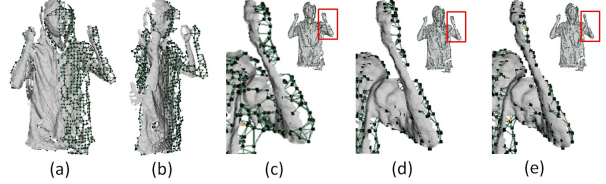


Figure 7. Compare only-nonrigid-registration with two-stage-registration.

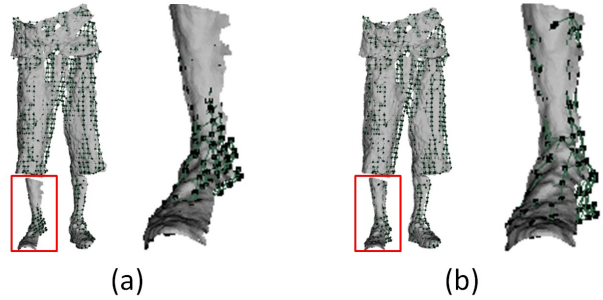


Figure 8. Comparison between correspondences without/with bijective consistence: (a) vs (b).

Relax-Regularization. Figure 9 shows that our relax regularization is able to adjust the integrated graph to correct position (Figure 9(a)), while the non-relax regularization is less flexible to deform the graph (Figure 9(b)).

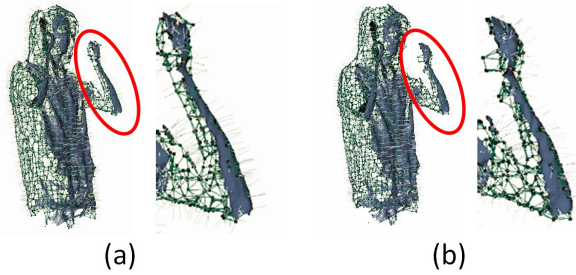


Figure 9. Comparison between relax regularization (a) and non-relax regularization (b).

6.2. More Results

We manually rotate a puppet and a pillow in front of a Kinect to capture the depth data. The hand-held rotation inevitably incurs deformation on the objects. Figure 10 and Figure 11 exhibit effectiveness of our method. In the two figures, the first rows are our results, and the second rows are results with rigid global registration. For clearness, we show phong-rendering and normal maps of these results under different views, and highlight the obvious artifacts with red rectangles.

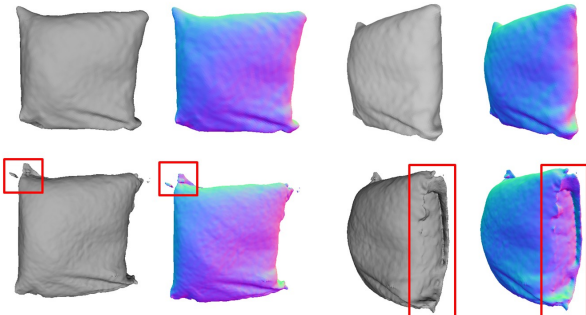


Figure 10. Comparison between our method and global rigid registration on the pillow.

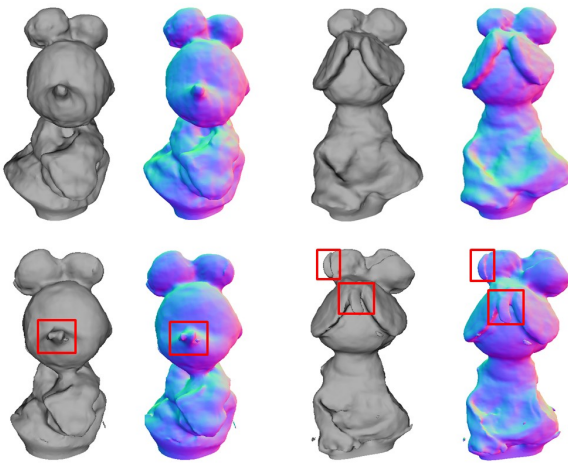


Figure 11. Comparison between our method and global rigid registration on the puppet.

6.3. Application: Human Body Modeling

Our method is suitable for building a human body modeling system. We fix two Kinect on a stand, one up and one down to capture upper and lower parts of a human body, respectively. Views of both Kinects overlap in a small region (as a prototype, we do not address the interference problem). To scan a human body, the human is asked to rotate by herself in front of the system, and try to keep her pose. During the process, the system captures depths of the movement. After capture, we independently run the pipeline for upper and lower parts, then merge their warped point cloud together, and finally use poisson reconstruction to get the model. It usually takes about 30 to 60 seconds to capture the depths, and about 10 minutes to generate the model. Figure 12 shows some results, where our method preserves necessary details, such as collars, small folders, face, and even the hood with complex topology. These results are pleasing regarding to the low price setup.

7. Conclusion

We have presented a general method for quasi-rigid shape modeling using depth scans captured at different time instances. In our method, to keep generality we do not require a template to assist the geometry tracking. Without the template, we gradually integrate depth scans into our pipeline and finally obtain a deformation graph representing the whole shape. The method is robust thanks to two key technique contributions. First is our model-to-part scheme to register the deformation graph to match the new scans. To keep the registration robust, we adopt a two-stage registration under the assumption of as-rigid-as-possible. Second, we handle several topology issues raised with the integration of depth scans. The special cares on topology proposed in the paper in one hand tackle the problem of re-appearing part, and in other hand adaptively regularize the registration process. We demonstrated that the proposed method by reconstructing several quasi-rigid objects. As an application, we showed that our method can be used to build a human body scanning system.

References

- [1] D. Anguelov, P. Srinivasan, D. Koller, S. Thrun, J. Rodgers, and J. Davis. SCAPE: shape completion and animation of people. *ACM Transactions on Graphics TOG*, 24(3):408–416, 2005.
- [2] P. J. Besl and N. D. McKay. A method for registration of 3-d shapes. *IEEE Trans. Pattern Anal. Mach. Intell.*, 14(2):239–256, Feb. 1992.
- [3] W. Chang and M. Zwicker. Automatic registration for articulated shapes. *Comput. Graph. Forum*, 27(5):1459–1468, 2008.
- [4] W. Chang and M. Zwicker. Range Scan Registration Using Reduced Deformable Models. *Computer Graphics Forum*, 28(2):447–456, 2009.
- [5] W. Chang and M. Zwicker. Global registration of dynamic range scans for articulated model reconstruction. *ACM Transactions on Graphics*, 30(3):1–15, 2011.
- [6] Y. Chen and G. Medioni. Object modeling by registration of multiple range images. *Image and Vision Computing (IVC)*, 10(3):145–155, 1992.
- [7] E. De Aguiar, C. Stoll, C. Theobalt, N. Ahmed, H.-P. Seidel, and S. Thrun. Performance capture from sparse multi-view video. *ACM Transactions on Graphics*, 27(3):1, 2008.
- [8] Q.-X. Huang, B. Adams, M. Wicke, and L. J. Guibas. Non-Rigid Registration Under Isometric Deformations. *Computer Graphics Forum*, 27(5):1449–1457, 2008.
- [9] M. Levoy, K. Pulli, B. Curless, S. Rusinkiewicz, D. Koller, L. Pereira, M. Ginzton, S. Anderson, J. Davis, J. Ginsberg, J. Shade, and D. Fulk. The digital michelangelo project: 3d scanning of large statues. *SIGGRAPH ’00*, pages 131–144, New York, NY, USA, 2000. ACM Press/Addison-Wesley Publishing Co.

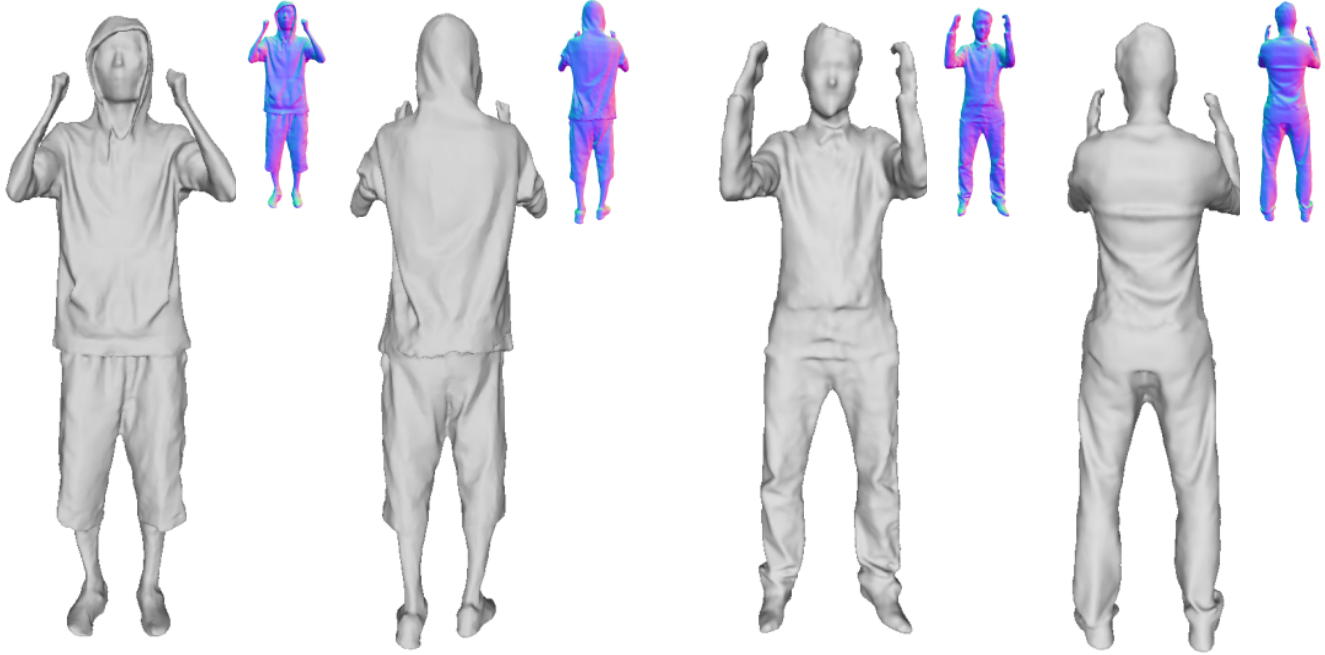


Figure 12. Results of human body modeling.

- [10] H. Li, B. Adams, L. J. Guibas, and M. Pauly. Robust single-view geometry and motion reconstruction. *ACM Transactions on Graphics*, 28(5):1, 2009.
- [11] H. Li, L. Luo, D. Vlasic, P. Peers, J. Popović, M. Pauly, and S. Rusinkiewicz. Temporally Coherent Completion of Dynamic Shapes. *ACM Transactions on Graphics*, 31(1), 2012.
- [12] H. Li, R. W. Sumner, and M. Pauly. Global correspondence optimization for non-rigid registration of depth scans. In *Proceedings of the Symposium on Geometry Processing*, SGP '08, pages 1421–1430, Aire-la-Ville, Switzerland, Switzerland, 2008. Eurographics Association.
- [13] M. L. M. Liao, Q. Z. Q. Zhang, H. W. H. Wang, R. Y. R. Yang, and M. G. M. Gong. Modeling deformable objects from a single depth camera. In *Proceedings of ICCV 2009*, number Iccv, pages 167–174. Ieee, 2009.
- [14] N. J. Mitra, S. Flöry, M. Ovsjanikov, N. Gelfand, L. Guibas, and H. Pottmann. Dynamic geometry registration. In *Proceedings of the fifth Eurographics symposium on Geometry processing*, SGP '07, pages 173–182, Aire-la-Ville, Switzerland, Switzerland, 2007. Eurographics Association.
- [15] R. A. Newcombe, S. Izadi, O. Hilliges, D. Molyneaux, D. Kim, A. J. Davison, P. Kohli, J. Shotton, S. Hodges, and A. Fitzgibbon. Kinectfusion: Real-time dense surface mapping and tracking. ISMAR '11, pages 127–136, Washington, DC, USA, 2011. IEEE Computer Society.
- [16] K. Pulli. Multiview registration for large data sets. 3DIM'99, pages 160–168, Washington, DC, USA, 1999. IEEE Computer Society.
- [17] S. Rusinkiewicz and M. Levoy. Efficient variants of the icp algorithm. In *3DIM'2001*, 2001.
- [18] G. C. Sharp, S. W. Lee, and D. K. Wehe. Multiview registration of 3d scenes by minimizing error between coordinate frames. *IEEE Trans. Pattern Anal. Mach. Intell.*, 26(8):1037–1050, Aug. 2004.
- [19] R. W. Sumner, J. Schmid, and M. Pauly. Embedded deformation for shape manipulation. *ACM Transactions on Graphics*, 26(3):80, 2007.
- [20] J. SÜssmuth, M. Winter, and G. U. Greiner. Reconstructing animated meshes from time-varying point clouds. *Computer Graphics Forum SGP 08*, 27(5), 2008.
- [21] N. Y. T. Masuda, K. Sakaue. Registration and integration of multiple range images for 3-d model construction. In *IEEE Conf. on Computer Vision and Pattern Recognition*, pages 879–883, June 1996.
- [22] A. R. T. Tevs, A. Berner, M. Wand, I. V. O. Ihrke, M. Bokeloh, J. Kerber, and H.-p. Seidel. Animation Cartography - Intrinsic Reconstruction of Shape and Motion. *ACM Transaction on Graphics TOG*, 31(2):15 pages, 2012.
- [23] J. Tong, J. Zhou, L. Liu, Z. Pan, and H. Yan. Scanning 3D full human bodies using Kinects. *IEEE TVCG*, 18(4):643–50, 2012.
- [24] D. Vlasic, P. Peers, I. Baran, P. Debevec, J. Popović, S. Rusinkiewicz, and W. Matusik. Dynamic shape capture using multi-view photometric stereo. *ACM Transactions on Graphics*, 28(5):174, 2009.
- [25] M. Wand, B. Adams, M. Ovsjanikov, A. Berner, M. Bokeloh, P. Jenke, L. Guibas, H.-P. Seidel, and A. Schilling. Efficient reconstruction of nonrigid shape and motion from real-time 3D scanner data. *ACM Transactions on Graphics*, 28(2):1–15, 2009.
- [26] A. Weiss, D. Hirshberg, and M. J. Black. Home 3D body scans from noisy image and range data. In *2011 International Conference on Computer Vision*, pages 1951–1958. IEEE, 2011.